Eur J Nucl Med Mol Imaging (2010) 37:67–77
DOI 10.1007/s00259-009-1205-y

ORIGINAL ARTICLE

Detection of unknown primary neuroendocrine tumours (CUP-NET) using ^{68}Ga-DOTA-NOC receptor PET/CT

Vikas Prasad · Valentina Ambrosini · Merten Hommann · Dieter Hoersch · Stefano Fanti · Richard P. Baum

Received: 30 November 2008 / Accepted: 12 June 2009 / Published online: 18 July 2009
© Springer-Verlag 2009

Abstract
Purpose This bi-centric study aimed to determine the role of receptor PET/CT using ^{68}Ga-DOTA-NOC in the detection of undiagnosed primary sites of neuroendocrine tumours (NETs) and to understand the molecular behaviour of the primarily undiagnosed tumours.
Methods Overall 59 patients (33 men and 26 women, age: 65±9 years) with documented NET and unknown primary were enrolled. PET/CT was performed after injection of approximately 100 MBq (46–260 MBq) of ^{68}Ga-DOTA-NOC. The maximum standardised uptake values (SUV_{max}) were calculated and compared with SUV_{max} in known pancreatic NET (pNET) and ileum/jejunum/duodenum (SI-NET). The results of PET/CT were also correlated with CT alone.
Results In 35 of 59 patients (59%), ^{68}Ga-DOTA-NOC PET/CT localised the site of the primary: ileum/jejunum (14), pancreas (16), rectum/colon (2), lungs (2) and paraganglioma (1). CT alone (on retrospective analyses) confirmed the findings in 12 of 59 patients (20%). The mean SUV_{max} of identified previously unknown pNET and SI-NET were 18.6±9.8 (range: 7.8–34.8) and 9.1±6.0 (range: 4.2–27.8), respectively. SUV_{max} in patients with previously known pNET and SI-NET were 26.1±14.5 (range: 8.7–42.4) and 11.3±3.7 (range: 5.6–17.9). The SUV_{max} of the unknown pNET and SI-NET were significantly lower ($p<0.05$) as compared to the ones with known primary tumour sites; 19% of the patients had high-grade and 81% low-grade NET. Based on ^{68}Ga-DOTA-NOC receptor PET/CT, 6 of 59 patients were operated and the primary was removed (4 pancreatic, 1 ileal and 1 rectal tumour) resulting in a management change in approximately 10% of the patients. In the remaining 29 patients, because of the far advanced stage of the disease (due to distant metastases), the primary tumours were not operated. Additional histopathological sampling was available from one patient with bronchial carcinoid (through bronchoscopy).
Conclusion Our data indicate that ^{68}Ga-DOTA-NOC PET/CT is highly superior to ^{111}In-OctreoScan (39% detection rate for CUP according to the literature) and can play a major role in the management of patients with CUP-NET.

Keywords Unknown primary · Neuroendocrine tumour · ^{68}Ga-DOTA-NOC · Receptor PET/CT · Molecular imaging

V. Prasad · R. P. Baum (✉)
Department of Nuclear Medicine and Centre for PET/CT,
Zentralklinik Bad Berka,
Robert Koch Allee-9,
99437 Bad Berka, Germany
e-mail: info@rpbaum.de

V. Ambrosini · S. Fanti
Nuclear Medicine Unit, Policlinico S. Orsola-Malpighi,
University of Bologna,
Bologna, Italy

M. Hommann
Department of General and Visceral Surgery,
Zentralklinik Bad Berka,
Bad Berka, Germany

D. Hoersch
Department of Internal Medicine/Gastroenterology,
Oncology and Endocrinology, Zentralklinik Bad Berka,
Bad Berka, Germany

Introduction

Carcinoma of unknown primary (CUP) is defined as a biopsy-proven secondary lesion without any evidence of primary site after physical examination and conventional

imaging tests (MRI, CT and US). The site of the occult primary tumour often remains unidentified after conventional imaging investigations (chest X-ray, abdominal and pelvic CT, mammography in women) (20–70% of cases) [1, 2] or autopsy (30–82%) [2–4] . Overall, in approximately 3% of the patients, the site of origin of a histologically documented carcinoma is not identified clinically [5–9]. Early identification of the primary tumour is a fundamental prerequisite for changing a patient's prognosis and prolonging the survival [10].

Whole-body PET/CT using ^{18}F-FDG has been successfully used for the detection of CUP of the most common malignancies, namely adenocarcinoma, squamous cell carcinoma and poorly differentiated carcinoma, identifying the primary lesion in 24–40% of patients [11–16]. However, the role of ^{18}F-FDG PET is limited in slowly growing tumours, such as well-differentiated neuroendocrine tumours (NET) [17]. Among the novel tracers that may provide a more accurate localisation of NET, ^{18}F-DOPA [18] and recently ^{68}Ga-DOTA-NOC [19, 20] have been suggested.

The aim of this bi-centric study was to evaluate the clinical usefulness of ^{68}Ga-DOTA-NOC receptor PET/CT in the identification of the primary tumour site in NET patients and to understand the molecular behaviour of primarily undiagnosed carcinomas.

Materials and methods

Fifty-nine patients with histologically proven NET and unknown primary tumour were enrolled at the Department of Nuclear Medicine/PET Centre, Bad Berka, Germany and at the Unit of Nuclear Medicine, S. Orsola-Malpighi Hospital, Bologna, Italy, between July 2004 and February 2007. Six patients were enrolled at the University Hospital in Bologna and the remaining 53 at the Zentralklinik in Bad Berka. This study was performed in accordance with German regulations (as published by the Federal Office for Radiation Protection, BfS) and approved by the Ethics Committee of the S. Orsola-Malpighi Hospital of Bologna. Each patient was extensively informed about the PET/CT procedure and possible adverse effects. Written informed consent was obtained from all patients.

The **inclusion criteria** were (1) biopsy-proven NET and (2) an unidentified primary tumour (negative physical examination and conventional imaging).

All patients underwent multislice CT, magnetic resonance imaging (MRI 1.5 T) and ultrasonography (USG). In patients with suspicion/evidence of primary in the pancreas, endosonography (EUS) was performed. The maximum time interval between last morphological imaging study (chest X-ray, CT and/or MRI or USG) and PET/CT was 3 weeks.

^{68}Ga-DOTA-NOC labelling

The elution of ^{68}Ga from ^{68}Ge/^{68}Ga generator (obtained from Eckert and Ziegler, Berlin, Germany) and its labelling and associated quality control were performed as described in a previous publication [21]. Shortly, preconcentration and purification of the initial generator eluate were performed using a miniaturised column with organic cation-exchanger resin and hydrochloric acid/acetone eluent. The purified fraction was used for the labelling of nanomolar amounts of octreotide derivatives either in pure aqueous solution or in buffers. Using the generator post-eluate processing system, >97% of the initially eluted ^{68}Ga activity was obtained within 4 min as a 0.4-ml volume of a hydrochloric acid/acetone fraction. The initial amount of ^{68}Ge (IV) was decreased by a factor of 10^4, whereas initial amounts of Zn(II), Ti(IV) and Fe(III) were reduced by factors of 10^5, 10^2 and 10, respectively. The processed ^{68}Ga fraction was directly transferred to solutions containing 30–50 μg of DOTA-NOC. Labelling yields of >95% were achieved within 10 min. Overall yields reached 70% at 20 min after generator elution relative to the eluted ^{68}Ga activity, not corrected for decay. ^{68}Ga labelling of DOTA-NOC was performed following the procedure described by Meyer et al. [22].

At the Zentralklinik Bad Berka, all patients were examined on a dual-modality PET/CT tomograph (biograph duo, Siemens Medical Solutions). The CT component of the biograph BGO duo corresponds to a Somatom Emotion Duo (Siemens Medical Solutions), a 2-row spiral CT system with a maximum continuous scan time of 100 s and a maximum rotation speed of 75 rpm. The PET components of the combined PET/CT tomograph are based on a full-ring lutetium orthosilicate (LSO) PET system. Although the CT images constructed out of the raw data from the PET/CT data were inferior to the diagnostic CT, the use of contrast agents and acquisition of CT images during the venous phase of the contrast agent assured that image quality was suitable for diagnostic purposes. At the S. Orsola-Malpighi Hospital of Bologna, patients were examined using a dedicated hybrid PET/CT tomograph (Discovery LS scanner, GE Medical Systems, Waukesha, WI, USA). The patients fasted 6 h before the scans were carried out (intravenous injection of 185 MBq ^{68}Ga-DOTA-NOC, uptake time 60 min). PET scan emission images were recorded for 4 min per bed position; for non-uniform attenuation correction, CT images were used (acquisition parameters: 140 kV, 90 mA, 0.8 s, tube rotation, 5 mm thickness). PET images were acquired from the skull base to the middle part of the thigh.

At the Zentralklinik Bad Berka, acquisition started 60–90 min after injection of approximately 100 MBq (46–260 MBq) ^{68}Ga-DOTA-NOC. Depending upon the severity

of symptoms in functionally active tumours (e.g. carcinoid syndrome), patients were either advised to stop octreotide therapy (if on treatment) 6 weeks prior to ^{68}Ga-DOTA-NOC PET/CT study when using a long-acting formulation [e.g. sandostatin long-acting repeatable (LAR) or somatuline] or in cases with severe symptoms, convert from LAR to s.c. application. All patients at Bad Berka were asked to drink 1.5 l of a water-equivalent oral contrast dispersion (Gastrografin). This dispersion is used routinely in PET/CT without known adverse side effects to the accumulation of ^{68}Ga-DOTA-NOC. Immediately before the PET/CT examination, patients were asked to void the bladder. Patients were positioned head first supine on the common patient handling system with the arms raised in accordance with standard CT practice.

First, a topogram was acquired over 1,024 mm axially. Coaxial whole-body imaging ranges were defined on the topogram, covering an area from the skull to the upper thighs (7–8 PET bed positions, or 90–100 cm, depending on the size of the patient). After 100 ml of intravenous contrast (by an automated injection pump) administration, contrast-enhanced CT was acquired in the craniocaudal direction with a 30-s delay. CT was performed in spiral mode using a continuous acquisition at 130 kVp, 115 mAs, 4-mm collimation, 5-mm slice width, a table feed of 8 mm per rotation at 0.8-s rotation time and 2.4-mm slice spacing. During the CT acquisition a limited breath-hold protocol was followed, which required the patients to hold their breath in normal expiration. After completion of the CT, patients were moved automatically to the PET toward the rear of the gantry, where two-dimensional PET emission scanning subsequently started in the caudocranial direction with the bladder/pelvis region being scanned first. An emission scan time of 1–**2** min per bed position was used for all patients (depending upon the patient's weight and height), which resulted in a total emission scan time of no more than 24 min and a total PET/CT examination time of about 30 min (including patient positioning, CT and PET imaging). In Bologna, the emission scan time was 2–4 min per bed position according to the scanner used (GE Discovery STE, GE Discovery LS), which resulted in a total emission scan time of no more than 12–24 min and a total PET/CT examination of about 30 min (including the PET/CT scan and patient positioning).

Data reconstruction and image analysis

The CT transmission images were used for attenuation correction of the PET emission data. After scatter and attenuation correction, PET emission data were reconstructed using an attenuation-weighted ordered subsets expectation maximisation approach with 2 iterations and 8 subsets on 128×128 matrices and with a 5-mm Gaussian post-reconstruction filtering.

At the Zentralklinik Bad Berka, image analysis of the CT was performed on a syngo viewing station by an experienced radiologist (more than 5 years of CT experience). The PET/CT images were assessed using the e.soft workstation (Siemens Medical Solutions) by two experienced nuclear medicine physicians. In Bologna, the PET/CT images were assessed using the GE Xeleris workstation (GE) by two experienced nuclear medicine physicians.

First, the maximum intensity projection (MIP) images were visually inspected in varying scales. Thereafter, each single transversal slice was viewed from head to mid-thigh in combination with the corresponding CT image and the fused image slice and each focal, abnormal tracer uptake was recorded by slice number and anatomical localisation. Finally, manually selected regions of interest (ROIs) were automatically drawn on a single slice of the reconstructed PET images using a 50% standardised uptake value (SUV) threshold and the software provided by e.soft. Any area with intensity greater than background that could not be explained by physiological activity was considered to be indicative of tumour tissue.

For semi-quantitative analysis SUV_{max} was calculated. However, because of the dependency of SUV_{max} on different PET scanners used at two centres, only the patients enrolled at the Zentralklinik Bad Berka were taken into consideration for comparison of the SUV_{max} of primary pancreatic NET and ilium/jejunum/duodenum with the SUV_{max} of known pancreatic NETs in 49 patients and that of known ileum/jejunum/duodenum NETs in 11 patients. The results of PET/CT were also correlated with CT alone. Histopathological confirmation was not possible in all of the cases. Hence, the lesions detected on ^{68}Ga-DOTA-NOC PET/CT were considered to be positive by follow-up for a minimum duration of 6 months with ^{68}Ga-DOTA-NOC PET/CT, ultrasound, biochemical markers or in the case of pancreatic lesions with EUS.

Statistical analyses

Statistical analysis was performed using dedicated statistical software. Correlation and significance levels were calculated using SPSS 13. Values were tested for significance applying the nonparametric Mann Whitney test for SUV. Because of the lack of normally distributed data, Spearman's rank correlation was used.

Results

^{68}Ga-DOTA-NOC PET/CT was performed in 59 patients with documented NET (confirmed on biopsy from metastatic lesions) and unknown primary tumour (Table 1). ^{68}Ga-DOTA-NOC PET/CT could localise the site of the

Table 1 Patients' characteristics

Age	65±9years
Male to female ratio	33:26
Primary tumour	Total detected: 35/59
	Pancreas, *n*=16
	Ileum/jejunum/duodenum, *n*=14
	Rectum/colon, *n*=2
	Lungs, *n*=2
	Paraganglioma, *n*=1
WHO classification	Well-differentiated, *n*=45
	Moderately differentiated, *n*=2
	Poorly differentiated, *n*=2
	Undifferentiated, *n*=2
	NA, *n*=8
pNET SUV_{max}	Previously known tumours: 26.1±14.5
	Previously unknown: 18.6±9.8
SI-NET SUV_{max}	Previously known: 11.3±3.7
	Previously unknown: 9.1±6.0
Ki-67 (*n*=22)	High-grade (Ki-67>15%): 4/22 (18%)
	Low-grade (Ki-67<2 %): 16/22 (73%)
	Intermediate-grade (Ki-67 5–15%): 2/22 (9%)

NA not available, *pNET* pancreatic neuroendocrine tumour, *SI-NET* small intestinal neuroendocrine tumours (ileum/jejunum/duodenum)

primary tumour in 35 of 59 (59%) at the following locations: pancreas: 16 (Figs. 1 and 2a), head: 5, body: 4, tail: 3, multifocal: 3, processus uncinatus: 1, lungs: 2 (Fig. 2a), rectum/colon: 2 (Fig. 2b), duodenum/ileum/jejunum: 14 (Fig. 2c) and paraganglioma: 1 (Table 2). Of 16 pancreatic lesions 5 also had CT correlation, 2 pancreatic lesions were confirmed on EUS (CT was negative) and in the other 2 patients there was indirect evidence/suspicion of tumour. Of five patients with tumour in the head region of the pancreas, one had gastrinoma

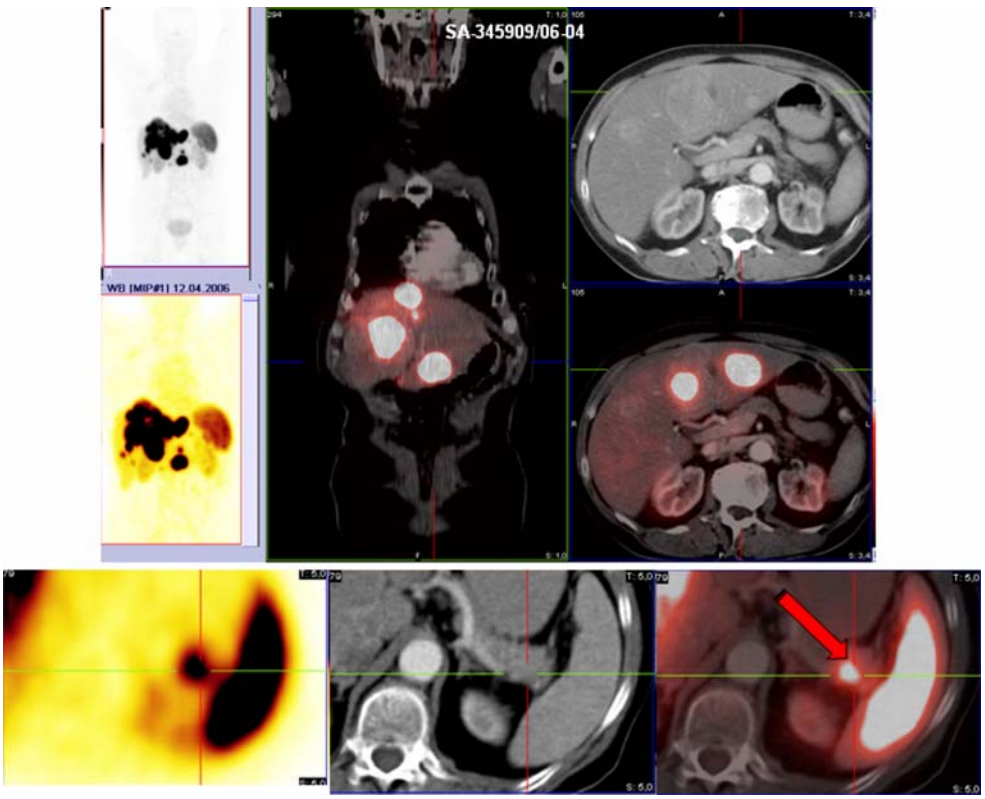

Fig. 1 Non-functional NET with multiple liver metastases (CUP syndrome). The primary tumour was detected by receptor PET/CT in the tail of the pancreas (*arrow*) and later confirmed by endoscopic ultrasound and biopsy

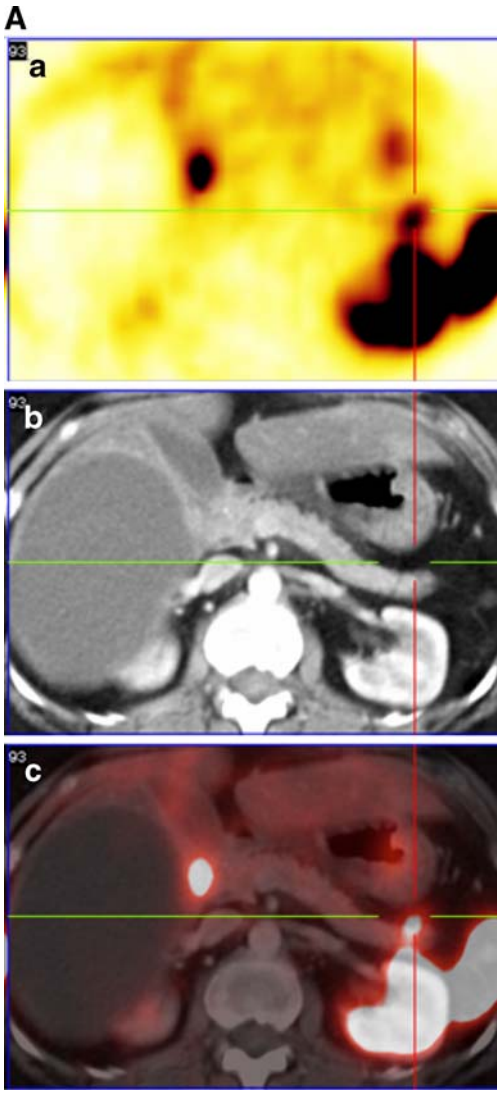

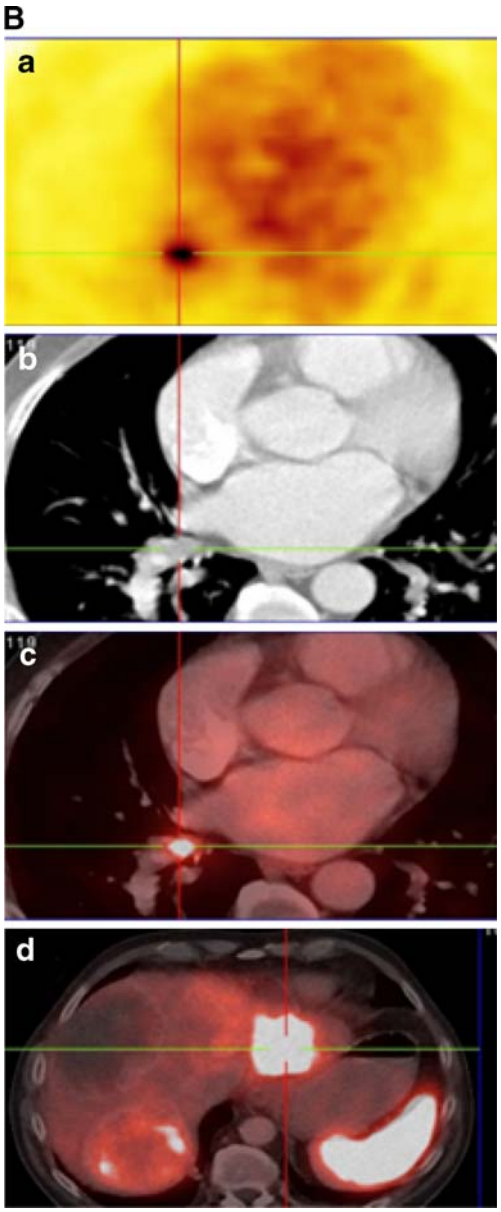

Fig. 2 **A** Multifocal primary pNET(in head and tail) detected on receptor PET/CT. EUS later confirmed the lesion in the head but missed the one in the pancreatic tail. **B** Patient with large liver metastases from a neuroendocrine tumour (unknown primary) referred for PRRT. Receptor PET/CT detected the primary in the right bronchus confirmed later on by bronchoscopy. a) ^{68}Ga-DOTA-NOC PET image, b) CT image, c) PET/CT fusion image, d) PET/CT fusion image of the liver lesions. **C** Neuroendocrine tumour patient with CUP referred for PRRT. ^{68}Ga-DOTA-NOC PET/CT revealed the primary in the rectum (*I*). Additionally, pararectal lymph node metastases were clearly detectable (*II*). The patient was referred for surgery. a) PET image, b) CT image, c) PET/CT fusion image. **D** Primary ileum neuroendocrine carcinoma without detection on receptor PET/CT. The patient was later on operated and the primary was resected

Fig. 2 (continued)

which was CT negative; persistent elevated gastrin level in follow-up confirmed the findings of PET/CT. In one patient there was indirect evidence of tumour in the pancreatic head/processus uncinatus region; one patient had EUS confirmation, while the fourth patient had CT correlation. Overall 80% (4/5) of the PET/CT findings of tumour in the pancreatic head were confirmed. CT alone confirmed the findings in 12 of 59 patients (20%). According to the WHO classification, 45 patients had well-differentiated endocrine carcinoma, 2 had moderately differentiated endocrine carcinoma, 2 had poorly differentiated endocrine carcinoma and 2 had undifferentiated endocrine carcinoma. In the remaining eight cases the WHO classification was not available (Fig. 3, Table 3).

The average time interval between the first biopsy-proven diagnosis of NET and the first evidence of primary on ^{68}Ga-DOTA-NOC receptor PET/CT was found to be approximately 29 months. CT alone (with knowledge of the PET results, Table 4) showed abnormal findings in 12 of 59 patients (20%). In 24 of 59 patients (41%), the primary remained undiagnosed, even after ^{68}Ga-DOTA-NOC receptor PET/CT.

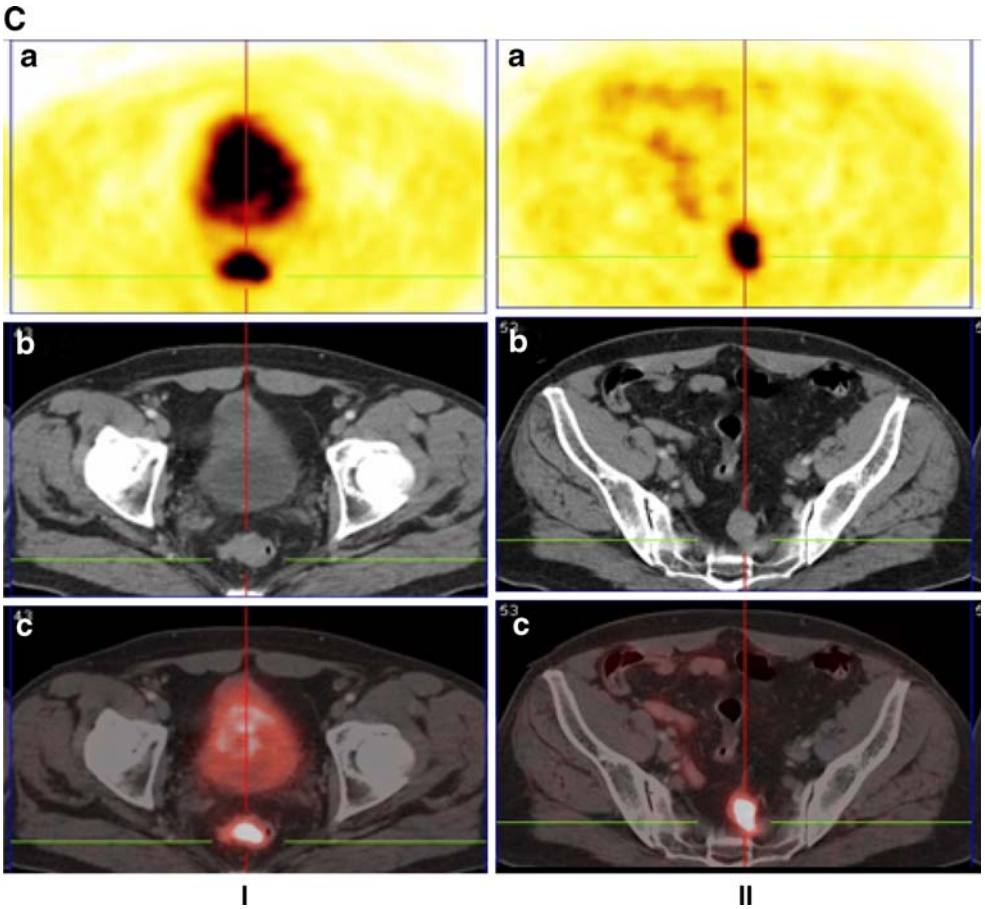

Fig. 2 (continued)

PET/CT with ^{68}Ga-DOTA-NOC identified lymph node metastases in 30 patients (only 16 of 30 were detected by CT), liver metastases in 46 cases (38 of 46 evident also on CT scan) and bone metastases in 17 cases (8 of 17 identified by CT). For the identification of the primary, ^{68}Ga-DOTA-NOC PET alone in many instances was not sufficient in giving the exact anatomical location; a PET/CT fusion image was required for the correct diagnosis. Also, some of the metastatic lesions in liver were picked up only on CT; however, no additional information regarding the site of the primary could be ascertained only on the basis of the CT scan.

In the patients enrolled at the PET Centre in Bad Berka, the SUV_{max} of the patients with CUP were compared with the SUV_{max} obtained in the other 49 patients with known pancreatic NET and in 11 patients with known ileum/jejunum/duodenum NET. The mean SUV_{max} of identified previously unknown primary pancreatic NET was 18.6±9.8 (range: 7.8–34.8) and 9.1±6.0 (range: 4.2–27.8) of SI-NET. SUV_{max} in patients with previously known pNET and SI-NET were 26.1±14.5 (range: 8.7–42.4) and 11.3±3.6 (range: 5.6–17.9). The SUV_{max} of the unknown pNET and SI-NET was significantly lower ($p<0.05$) as compared to the ones with known primary tumour. One of the patients had an SUV_{max} of 27.8 (Ileal NET)—the primary of this patient was diagnosed 11 years after the first histopathological correlation from liver lesions.

The Ki-67 values (proliferation index) were available in 22 of 59 patients: 4 of 22 patients (18%) had high-grade NET (Ki-67 value>15%), 16 of 22 (73%) low-grade NET (Ki-67< 5%) and 2 of 22 (9%) had Ki-67 in between 5 and 15%.

Based on ^{68}Ga-DOTA-NOC receptor PET/CT, 6 of 59 patients were operated and the primary was removed (4 pancreatic, 1 ileal and 1 rectal tumour) resulting in a management change in approximately 10% of the patients. In the remaining 29 patients, because of the far advanced stage of the disease (due to distant metastases), the primary tumours were not operated. Additional histopathological sampling was available from one patient with one bronchial carcinoid (through bronchoscopy).

Discussion

The majority of CUP are adenocarcinomas or undifferentiated tumours and less commonly, squamous cell carcinoma, melanoma or sarcoma; neuroendocrine tumours frequently present with a primary site of origin that cannot be determined [23].

In a retrospective review of 657 consecutive patients with CUP, Abbruzzese et al. reported several variables of

Fig. 2 (continued)

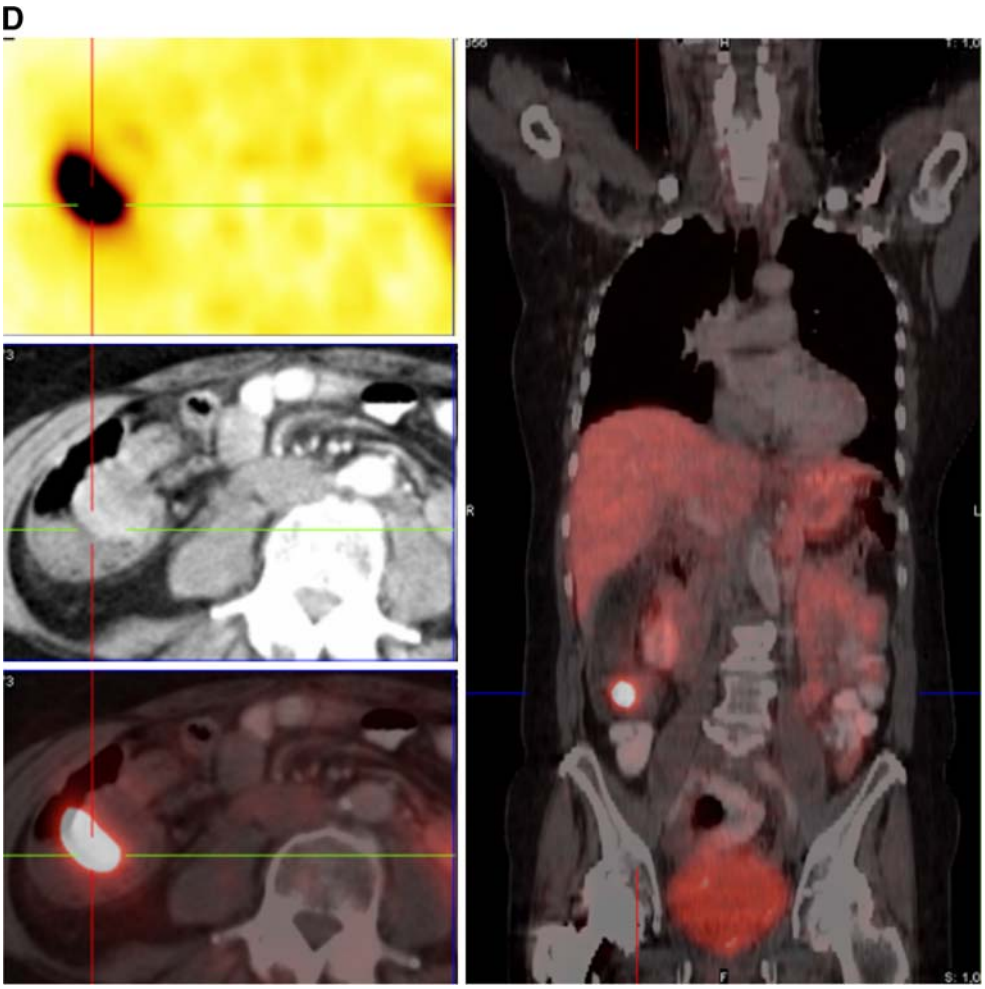

significant prognostic importance identified by multivariate analysis. Lymph node involvement and neuroendocrine histology were found to be associated with longer survival; male sex, increasing number of involved organ sites, adenocarcinoma histology and hepatic involvement were unfavourable prognostic factors [24].

The prognosis of patients with CUP is poor. As a group, the median survival is reported to be approximately 3–4 months with less than 25 and 10% of patients alive at 1 and 5 years, respectively [23, 25–27]. A literature survey shows that the detection of the primary tumour site prolongs survival (for about 1–2 years) [10]. FDG PET has been reported to be useful for the detection of the primary tumour in patients with a negative diagnostic work-up. However, until now, no systematic study has been performed to

Table 2 Comparison of the sensitivity of ^{68}Ga-DOTA-NOC PET/CT and CT alone for detection of the primary tumour and sites of metastases of neuroendocrine tumours

Site	^{68}Ga-DOTA-NOC PET/CT	CT
Primary tumour	35/59 (59%)	12/59 (20%)
Liver metastases	46/59 (78%)	38/59 (64%)
Lymph node metastases	30/59 (51%)	16/69 (27%)
Bone metastases	17/59 (29%)	8/59 (14%)
Lung metastases	3/59 (5%)	3/59 (5%)

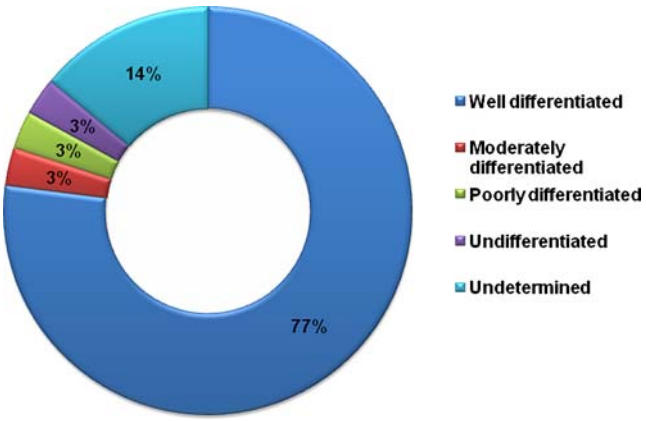

Fig. 3 WHO classification of the previously unknown primary neuroendocrine tumours detected on ^{68}Ga-DOTA-NOC PET/CT

Table 3 Different primary tumours detected and their Ki-67, WHO classification and positivity on CT

Patient number	Diagnosis/site	WHO classification	Ki-67	CT
Zentralklinik Bad Berka				
1	Pancreas tail	Undifferentiated	15%	
2	Unknown	Unknown		
3	Unknown	Well-differentiated		
4	Unknown	Well-differentiated		
5	Unknown	Unknown	<3%	
6	Pancreas tail	Well-differentiated	<3%	+ve
7	Pancreas body	Poorly differentiated	70%	+ve
8	Unknown	Well-differentiated		
9	Unknown	Moderately differentiated	40%	
10	Pancreas body	Undifferentiated	30%	+ve
11	Pancreas head	Well-differentiated	8%	+ve
12	Unknown	Well-differentiated		
13	Multifocal jejunum	Well-differentiated		
14	Jejunum	Well-differentiated		
15	Unknown	Unknown		
16	Ileum	Well-differentiated		
17	Unknown	Well-differentiated		
18	Ileum and jejunum	Well-differentiated	<2%	
19	Ileum	Well-differentiated		+ve
20	Pancreas multifocal	Well-differentiated	3%	
21	Lingula lungs	Well-differentiated		+ve
22	Pancreas body	Well-differentiated	3%	+ve
23	Unknown	Well-differentiated		
24	Unknown	Unknown		
25	Unknown	Well-differentiated	<1%	
26	Unknown	Unknown		
27	Ileum	Moderately differentiated		+ve
28	Jejunum	Well-differentiated		
29	Unknown	Unknown		
30	Unknown	Well-differentiated		
31	Unknown	Well-differentiated		
32	Lung (bronchus)	Well-differentiated		
33	Pancreas processus uncinatus	Well-differentiated		Indirect evidence
34	Pancreas head with physiological uptake in processus uncinatus	Well-differentiated		
35	Rectum	Well-differentiated	<2%	
36	Unknown	Well-differentiated	2%	
37	Ileum	Well-differentiated	2%	+ve
38	Pancreas head	Well-differentiated	<5%	
39	Gastrinoma (pancreas head)	Well-differentiated	<10%	
40	Unknown	Well-differentiated		
41	Pancreas head and body	Well-differentiated		+ve
42	Pancreas tail	Well-differentiated		
43	Duodenum, rectum, jejunum	Well-differentiated		
44	Colon	Well-differentiated	2%	
45	Unknown	Unknown		
46	Ileum	Well-differentiated		
47	Ileum	Well-differentiated		
48	Ileum	Well-differentiated	<5%	

Table 3 (continued)

Patient number	Diagnosis/site	WHO classification	Ki-67	CT
49	Paraganglioma	Well-differentiated		+ve
50	Small intestine	Well-differentiated		
51	Ileum	Well-differentiated	5%	
52	Unknown	Well-differentiated		
53	Unknown	Unknown	5%	
University of Bologna				
54	Pancreas head	Poorly differentiated		
55	Duodenum	Well-differentiated		
56	Unknown	Well-differentiated		
57	Pancreas body	Well-differentiated	2%	
58	Pancreas head and body	Well-differentiated		
59	Unknown	Well-differentiated	2%	

determine the incidence and clinical course of unknown primary in patients with neuroendocrine tumours [28, 29].

Numerous factors are known to have an influence on the survival and prognosis of patients with neuroendocrine tumours, among which the presence of liver metastases is the single most important factor. A correlation has been found between the size of the primary tumour and the probability of metastases for small intestinal carcinoids. Metastases to the liver can be found in 15–25% of tumours if the tumour diameter is less than 1 cm, 58–80% if it is 1–2 cm and more than 75% if the tumour size is more than 2 cm [28]. This makes it even more important to detect the primary tumour at the earliest stage. Surgery remains one of the treatment options with palliative as well curative intent (if performed at a stage when the primary is completely resectable or if there are no or few metastases) [28]. In the absence of any concrete evidence of primary on conventional imaging, exploratory laparotomy (for unknown gastroenteropancreatic neuroendocrine tumours) becomes more challenging. In this study, the detection of primaries could lead to the surgical removal in 10% of the cases. Of the four pancreatic NETs resected, one had no evidence of any lymph node, bone or liver metastases. Two patients had only peripancreatic lymph nodes. The fourth patient had both lymph node and liver metastases but still the surgeons decided to remove the primary. One patient was primarily referred for peptide receptor radionuclide therapy (PRRT) after chemotherapy. ^{68}Ga-DOTA-NOC PET/CT revealed only faint somatostatin receptor expression in the liver metastases (negative on CT) along with multiple necrotic lesions; the primary was detected in the rectum, along with presacral lymph nodes. Based upon these findings, the patient was referred for surgery. Another patient who had peritoneal and liver metastases was diagnosed with a primary tumour in the ileum. The primary was removed and the liver metastases were subsequently treated with PRRT. Somatostatin receptor PET/CT has been shown to be superior to ^{111}In-OctreoScan, the currently accepted gold standard in the diagnosis of NET [30]. However, ^{111}In-OctreoScan SPECT alone often fails in localising the exact site of the primary tumour (if detected) because of lack of morphological/anatomical information. ^{111}In-OctreoScan SPECT/CT overcomes some of these challenges; however, the sensitivity and resolution of gamma camera imaging is inferior to PET.

Table 4 Primary tumours found on CT after retrospective analyses of PET results

Primary site	CT positive
Small intestine (duodenum, ilium and jejunum)	2/14 (14.3%)
Pancreas	8/16 (50%)
Lungs (bronchus)	1/2 (50%)
Paraganglioma	1/1 (100%)
Overall	12/35 (34%)

Affinity for a broader spectrum of somatostatin receptor subtypes (SSTR 2, 3 and 5) makes ^{68}Ga-DOTA-NOC an interesting radiotracer for the detection of neuroendocrine tumours [31–33]. Our results, for the first time, have clearly shown that ^{68}Ga-DOTA-NOC receptor PET/CT fusion imaging is not only sensitive, but also highly specific in picking up the unknown primary. The sensitivity of receptor PET/CT was roughly three times higher as compared to CT alone. When compared to the literature [34], the detection rate of ^{68}Ga-DOTA-NOC was found to be much higher than for ^{111}In-OctreoScan (35% as compared to 59% for ^{68}Ga-DOTA-NOC PET). One of the probable explanations for the inability of ^{68}Ga-DOTA-NOC receptor PET/CT to pick up the primary—even when metastatic lesions are detected—is the sometimes extremely small size of the primary tumour or receptor down-regulation due to prolonged somatostatin therapy (e.g. using LAR

octreotide). The average time interval between the first biopsy-proven diagnosis of NET and the first evidence of primary on ^{68}Ga-DOTA-NOC receptor PET/CT was ~29 months. It may be hypothesised that the metastatic lesions, being comparatively new as compared to the primary, are subject to less intense down-regulation of receptors [35]. Also, the different degree of differentiation (different biological behaviour, e.g. growth rate) of the primary tumour and the metastatic lesions may account for the absence of somatostatin receptor positivity of the primary on PET/CT.

Our data also clearly suggest that for proper staging of NET and also for the follow-up, it is more appropriate to use ^{68}Ga-DOTA-NOC receptor PET/CT rather than CT or ^{68}Ga-DOTA-NOC PET alone. The addition of morphological information from CT was found to be absolutely essential in pinpointing the exact site of the primary tumour, particularly in the abdominal region.

Most of the patients had low-grade NET (Ki-67<5%), suggesting that low-grade NET is more common in patients with unknown primary. However, it is also important to remember that the natural history of differentiated NET is mostly indolent and that most of the NETs are of low grade. The degree of somatostatin receptor expression (as defined by SUV_{max}) suggests that patients with initially undiagnosed primary have a lower density of SSTR (for pancreatic tumours) as compared to the ones with known primary. This might be due to the different degree of differentiation as well as to the receptor down-regulation due to prolonged octreotide therapy [35]. NET of the small intestine remain the most difficult amongst all to be diagnosed by imaging modalities other than receptor PET/CT as was evident by the observation that CT could pick up primaries in these location in only 4 of 14 cases (29%), whereas at the same time 37% of the pancreatic lesions could be picked up by CT scan.

Surgical resection is one of the main treatments of primary neuroendocrine tumours, even if metastases are present (e.g. to avoid bowel obstruction or ileus). By using receptor PET/CT, it is possible to detect and remove the primary and hence to probably prolong survival and quality of life (e.g. by reduction of functional symptoms). Since receptor down-regulation/dedifferentiation of NET (e.g. in paraganglioma [36, 37]) with time is a known phenomenon, it may be possible that the induction of ^{68}Ga-DOTA-NOC (or other somatostatin receptor analogues labelled with positron emitters) early during the course of diagnostic work-up will improve the overall survival and quality of life.

One of the major drawbacks of this study is the lack of histopathological confirmation in most of the cases. It would be highly interesting to correlate the SSTR subtype in primary tumour with SUV_{max} [38], the degree of differentiation and Ki-67. It is also important to note that the normal physiological distribution of ^{68}Ga-DOTA-NOC in the processus uncinatus of the pancreas often poses a diagnostic challenge. In cases of a high degree of suspicion these patients should undergo EUS to confirm or rule out the primary tumour in the pancreatic head [39]. CT morphological information is also helpful in such cases. One of the patients in this study showed focal uptake of ^{68}Ga-DOTA-NOC in the processus uncinatus of the pancreas (SUV_{max} 11.7). CT in this patient although it did not show any definite evidence of mass lesion in the head showed evidence of atrophy of the pancreas cauda and tail with dilated ductus pancreaticus indirectly suggestive of a lesion in the pancreas head. In another patient, there was evidence of increased uptake in the head (primary tumour 9.1) and processus uncinatus (physiological SUV_{max} 4.7) of the pancreas. The results were confirmed by the EUS. CT findings did not show any mass lesion.

Another limitation of this study is that the SUV_{max} were not corrected for the size of the lesion to rule out partial volume effect as shown by Wieder et al. [40].

More studies are needed to ascertain the exact cause of failure to pick up an unknown primary tumour by receptor PET/CT and whether a combination of metabolic (^{18}F-DOPA or ^{18}F-FDG) and receptor PET/CT studies could further improve the detection rate.

References

1. Abbruzzese JL, Abbruzzese MC, Lenzi R, Hess KR, Raber MN. Analysis of a diagnostic strategy for patients with suspected tumors of unknown origin. J Clin Oncol 1995;13:2094–103.
2. Le Chevalier T, Cvitkovic E, Caille P, Harvey J, Contesso G, Spielmann M, et al. Early metastatic cancer of unknown primary origin at presentation. A clinical study of 302 consecutive autopsied patients. Arch Intern Med 1988;148:2035–9.
3. Didolkar MS, Fanous N, Elias EG, Moore RH. Metastatic carcinomas from occult primary tumors. A study of 254 patients. Ann Surg 1977;186:625–30.
4. Steckel RJ, Kagan AR. Diagnostic persistence in working up metastatic cancer with an unknown primary site. Radiology 1980;134:367–9.
5. Briasoulis E, Pavlidis N. Cancer of unknown primary origin. Oncologist 1997;2:142–52.
6. Hainsworth JD, Greco FA. Treatment of patients with cancer of an unknown primary site. N Engl J Med 1993;329:257–63.
7. McCredie M, Coates M, Churches T, Taylor R. Cancer incidence in New South Wales, Australia. Eur J Cancer 1991;27:928–31.
8. Muir C, Weiland L. Upper aerodigestive tract cancers. Cancer 1995;75:147–53.
9. Pavlidis N, Briasoulis E, Hainsworth J, Greco FA. Diagnostic and therapeutic management of cancer of an unknown primary. Eur J Cancer 2003;39:1990–2005.
10. Raber MN, Faintuch J, Abbruzzese JL, Sumrall C, Frost P. Continuous infusion 5-fluorouracil, etoposide and cis-diamminedichloroplatinum in patients with metastatic carcinoma of unknown primary origin. Ann Oncol 1991;2:519–20.
11. Syed R, Bomanji JB, Nagabhushan N, Hughes S, Kayani I, Groves A, et al. Impact of combined (18)F-FDG PET/CT in head and neck tumours. Br J Cancer 2005;92:1046–50.

12. Alberini JL, Belhocine T, Hustinx R, Daenen F, Rigo P. Whole-body positron emission tomography using fluorodeoxyglucose in patients with metastases of unknown primary tumours (CUP syndrome). Nucl Med Commun 2003;24:1081–6.
13. Bohuslavizki KH, Klutmann S, Kröger S, Sonnemann U, Buchert R, Werner JA, et al. FDG PET detection of unknown primary tumors. J Nucl Med 2000;41:816–22.
14. Freudenberg LS, Fischer M, Antoch G, Jentzen W, Gutzeit A, Rosenbaum SJ, et al. Dual modality of 18F-fluorodeoxyglucose-positron emission tomography/computed tomography in patients with cervical carcinoma of unknown primary. Med Princ Pract 2005;14:155–60.
15. Gutzeit A, Antoch G, Kühl H, Egelhof T, Fischer M, Hauth E, et al. Unknown primary tumors: detection with dual-modality PET/CT—initial experience. Radiology 2005; 234:227–34.
16. Kole AC, Nieweg OE, Pruim J, Hoekstra HJ, Koops HS, Roodenburg JL, et al. Detection of unknown occult primary tumors using positron emission tomography. Cancer 1998;82:1160–6.
17. Adams S, Baum R, Rink T, Schumm-Dräger PM, Usadel KH, Hör G. Limited value of fluorine-18 fluorodeoxyglucose positron emission tomography for the imaging of neuroendocrine tumours. Eur J Nucl Med 1998;25:79–83.
18. Ambrosini V, Tomassetti P, Rubello D, Campana D, Nanni C, Castellucci P, et al. Role of 18F-dopa PET/CT imaging in the management of patients with 111In-pentetreotide negative GEP tumours. Nucl Med Commun 2007;28:473–7.
19. Baum RP, Prasad V, Hommann M, Hörsch D. Receptor PET/CT imaging of neuroendocrine tumors. Recent Results Cancer Res 2008;170:225–42.
20. Ambrosini V, Tomassetti P, Castellucci P, Campana D, Montini G, Rubello D, et al. Comparison between 68Ga-DOTA-NOC and 18F-DOPA PET for the detection of gastro-entero-pancreatic and lung neuro-endocrine tumours. Eur J Nucl Med Mol Imaging 2008;35:1431–8.
21. Zhernosekov KP, Filosofov DV, Baum RP, Aschoff P, Bihl H, Razbash AA, et al. Processing of generator-produced 68Ga for medical application. J Nucl Med 2007;48:1741–8.
22. Meyer GJ, Macke H, Schuhmacher J, Knapp WH, Hofmann M. 68Ga-labelled DOTA-derivatised peptide ligands. Eur J Nucl Med Mol Imaging 2004;31:1097–104.
23. Neumann KH, Nystrom JS. Metastatic cancer of unknown origin: nonsquamous cell type. Semin Oncol 1982;9:427–34.
24. Abbruzzese JL, Abbruzzese MC, Hess KR, Raber MN, Lenzi R, Frost P. Unknown primary carcinoma: natural history and prognostic factors in 657 consecutive patients. J Clin Oncol 1994;12:1272–80.
25. Altman E, Cadman E. An analysis of 1539 patients with cancer of unknown primary site. Cancer 1986;57:120–4.
26. Moertel CG, Reitemeier RJ, Schutt AJ, Hahn RG. Treatment of the patient with adenocarcinoma of unknown origin. Cancer 1972;30:1469–72.
27. Ringenberg QS. Tumors of unknown origin. Med Pediatr Oncol 1985;13:301–6.
28. Jensen RT. Endocrine tumors of the gastrointestinal tract and pancreas. In: Kasper DL, Fauci AS, Longo DL, et al., editors. Harrison's principles of internal medicine. 16th ed. New York: McGraw-Hill; 2005
29. Rufini V, Calcagni ML, Baum RP. Imaging of neuroendocrine tumors. Semin Nucl Med 2006;36:228–7.
30. Gabriel M, Decristoforo C, Kendler D, Dobrozemsky G, Heute D, Uprimny C, et al. 68Ga-DOTA-Tyr3-octreotide PET in neuroendocrine tumors: comparison with somatostatin receptor scintigraphy and CT. J Nucl Med 2007;48:508–18.
31. Wild D, Mäcke HR, Waser B, Reubi JC, Ginj M, Rasch H, et al. 68Ga-DOTANOC: a first compound for PET imaging with high affinity for somatostatin receptor subtypes 2 and 5. Eur J Nucl Med Mol Imaging 2005;32:724.
32. Wild D, Schmitt JS, Ginj M, Mäcke HR, Bernard BF, Krenning E, et al. DOTA-NOC, a high-affinity ligand of somatostatin receptor subtypes 2, 3 and 5 for labelling with various radiometals. Eur J Nucl Med Mol Imaging 2003;30:1338–47.
33. Hofmann M, Maecke H, Börner R, Weckesser E, Schöffski P, Oei L, et al. Biokinetics and imaging with the somatostatin receptor PET radioligand (68)Ga-DOTATOC: preliminary data. Eur J Nucl Med 2001;28:1751–7.
34. Savelli G, Lucignani G, Seregni E, Marchianò A, Serafini G, Aliberti G, et al. Feasibility of somatostatin receptor scintigraphy in the detection of occult primary gastro-entero-pancreatic (GEP) neuroendocrine tumours. Nucl Med Commun 2004;25:445–9.
35. Hofland LJ, Lamberts SW. The pathophysiological consequences of somatostatin receptor internalization and resistance. Endocr Rev 2003;24:28–47.
36. Eisenhofer G, Siegert G, Kotzerke J, Bornstein SR, Pacak K. Current progress and future challenges in the biochemical diagnosis and treatment of pheochromocytomas and paragangliomas. Horm Metab Res 2008;40:329–37.
37. Mundschenk J, Unger N, Schulz S, Höllt V, Schulz S, Steinke R, et al. Somatostatin receptor subtypes in human pheochromocytoma: subcellular expression pattern and functional relevance for octreotide scintigraphy. J Clin Endocrinol Metab 2003;88:5150–7.
38. Miederer M, Seidl S, Buck A, Scheidhauer K, Wester HJ, Schwaiger M, et al. Correlation of immunohistopathological expression of somatostatin receptor 2 with standardised uptake values in 68Ga-DOTATOC PET/CT. Eur J Nucl Med Mol Imaging 2009;36:48–52.
39. Zimmer T, Scherübl H, Faiss S, Stölzel U, Riecken EO, Wiedenmann B. Endoscopic ultrasonography of neuroendocrine tumours. Digestion 2000;62(Suppl 1):45–50.
40. Wieder H, Beer AJ, Poethko T, Meisetschlaeger G, Wester HJ, Rummeny E, et al. PET/CT with Gluc-Lys-([(18)F]FP)-TOCA: correlation between uptake, size and arterial perfusion in somatostatin receptor positive lesions. Eur J Nucl Med Mol Imaging 2008;35:264–271.